Near-infrared transitions in iron-based diluted magnetic semiconductors: Effect of strong electron-phonon coupling

Vincenzo Savona and Franco Bassani
Scuola Normale Superiore, Pisa, Italy

Sergio Rodriguez
Department of Physics, Purdue University, West Lafayette, Indiana 47907-1396

(Received 15 July 1993)

We present a study of the effect of strong electron-phonon coupling on the levels of the ^{5}D term of Fe^{2+} in II-VI zinc-blende semiconductors. The nonperturbative approach leads to a dramatic decrease of the level spacings of the $^5\Gamma_5$ manifold of Fe^{2+} in a tetrahedral environment. The results allow us to propose a mechanism for those absorption lines in the excitation spectrum of Fe^{2+} in CdTe which are not attributed to zero-phonon lines deduced from crystal-field theory. It is also shown that transitions between the crystal-field split states of Fe^{2+} can be explained on the basis of mixing of $3d^6$ states with odd-parity states of higher configurations.

I. INTRODUCTION

The optical properties of transition-metal ions in II-VI compounds have been the object of many studies[1] since the 1960s. In the past decade, this subject has received renewed attention as part of a program of investigations on the optical and magnetic properties of alloys of II-VI semiconductors, denoted here by AB, with compounds of the form MB; here A and B are elements of the second and sixth columns of the Periodic Chart of the elements, respectively, and M is a transition metal of the iron group. The resulting alloys are described by the formula $A_{1-x}M_xB$ and are called diluted magnetic semiconductors[2] (DMS's).

Even though the results of this paper are concerned with the interpretation of the near-infrared absorption spectrum of a specific DMS, namely $Cd_{1-x}Fe_xTe$, for $x \ll 1$, the methods used are applicable to other DMS's. Studies of this material have been carried out by Slack, Roberts, and Vallin,[1] by Slack, Ham, and Chrenko[3] and, more recently, by Udo *et al.*[4] The present work contains two parts. The first gives an estimate of the oscillator strengths of near infrared transitions between states originating from the lowest term of Fe^{2+} modified by the effect of the crystal potential. The second deals with an alternative interpretation of some of the near-infrared lines observed in $Cd_{1-x}Fe_xTe$ which were ascribed to Fe^{2+} complexes in Ref. 4.

The lowest-energy term, ^5D, of Fe^{2+} substituting a Cd atom in CdTe is subjected to an electrostatic field (crystal potential) of tetrahedral symmetry[5] (point symmetry T_d). Since the crystal field is much stronger than the spin-orbit interaction, neglecting the latter leads to a splitting of the ^5D term into a $^5\Gamma_3$ orbital doublet and a $^5\Gamma_5$ orbital triplet, the former having lower energy than the latter. The spin-orbit interaction splits these manifolds further as follows. The tenfold $^5\Gamma_3$ separates into five approximately equidistant levels of symmetries Γ_1, Γ_4, Γ_3, Γ_5, and Γ_2, listed here in order of increasing energy. Similarly, the fifteenfold manifold $^5\Gamma_5$ splits into Γ_5, Γ_4, Γ_3, Γ_5, Γ_4, and Γ_1 levels also listed in order of increasing energy. The calculations of the energy spectrum just described have been carried out[1] within the framework of the crystal-field theory, the energies of the different levels being characterized by two parameters[6]: the crystal field splitting, Δ, and the strength of the spin-orbit interaction λ. Here $\Delta = E_\epsilon - E_\gamma$ is the energy separation of the $^5\Gamma_5(\epsilon)$ and $^5\Gamma_3(\gamma)$ multiplets prior to the introduction of the spin-orbit interaction.

The crystal-field splitting can be described by a single parameter because the T_d symmetry of the magnetic ion site requires that the crystal potential around the Fe^{2+} ion be of the form

$$V(\mathbf{r}) = a_3' xyz + a_4'(x^4+y^4+z^4-\tfrac{3}{5}r^4) + \cdots \tag{1}$$

where the terms omitted are polynomials in powers of x,y,z higher than four. The coordinates x,y,z are the projections of the position vector on the cubic axes of the CdTe zinc-blende structure. A constant term, giving rise to uniform shifts of the energy levels, has been disregarded. The perturbation on the Fe^{2+} ion is, of course, $\sum_a V(\mathbf{r}_a)$ where the sum extends over all the electrons in the ion. The matrix elements of the cubic term $\sum_a x_a y_a z_a$ vanish between any two states in the $3d^6$ configuration because of their even parity. Thus, a_3' contributes to the crystal-field splitting only in second order arising from mixing into the $3d^6$ states those from configurations having odd parity. In Sec. II we investigate the significance of this mixing in the explanation of the mechanism of optical absorption between the perturbed $3d^6$ states. The fourth-order potential has nonvanishing matrix elements between $3d^6$ states but terms of sixth and higher powers in the coordinates yield zero matrix elements by virtue of the Wigner-Eckart theorem.

The parameter Δ is directly proportional to a_4' and is given by

$$\Delta=-(4a_4'/21)\langle r^4\rangle \ , \tag{2}$$

where $\langle r^4\rangle$ is the average of the fourth power of the radius vector over the $3d$ radial wave function of the ion. Within the framework of the point ion hypothesis, taking only the four nearest-neighbor anions into account,

$$a_4'=-(35ze^2/9R^5) \ , \tag{3}$$

where z is the effective charge on the anions and R the anion-cation distance ($R=2.8$ Å in CdTe). Taking $z=2$ and $\langle r^4\rangle=4.496$ atomic units[7,8] we find $\Delta=352$ cm^{-1}. Experiments[1,4] show that $\Delta\approx2470$ cm^{-1} indicating that CdTe is only partly ionic and possesses a significant covalent electron density between anions and cations. This matter will receive additional attention in Sec. II.

Section II is devoted to an analysis of the optical transitions between levels in the $^5\Gamma_3$ and $^5\Gamma_5$ manifolds and, in particular, to the comparison of the experimentally estimated oscillator strengths with those predicted by theory. We conclude that the transitions observed in the near infrared are electric-dipole-induced by mixing of the $3d^6$ and higher, odd-parity, configurations. This result is in agreement with the relative intensities deduced from symmetry considerations alone discussed in Ref. 4.

In Sec. III we investigate the interaction of the $3d$ electronic states of the Fe^{2+} ion and the vibrations of the crystal. The lattice vibrations will be classified according to the irreducible representations of the symmetry group of orthogonal transformations around the magnetic ion rather than according to the space group of the crystal. In this manner, each mode is a superposition of phonons belonging to different points of the fundamental Brillouin zone (BZ) of the crystal. These points are obtained from one another by application of the operations of the point group of the cation site. Thus, each mode considered here belongs to a star of values of the wave vector within the BZ. The decomposition of the phonon modes according to the point group T_d for a few high symmetry points of the zinc-blende BZ is given in Table I where we also list the corresponding phonon frequencies for CdTe.

The main purpose of Sec. III is to discuss the interpretation of those near-infrared absorption lines in $Cd_{1-x}Fe_xTe$ which cannot be accounted for purely within the framework of crystal-field theory. They are reported in Refs. 1 and 4 and are labeled $X_{\rm I}$ and Y in the latter (see Fig. 3 of Ref. 4); their origin was tentatively attributed to the formation of Fe^{2+} complexes such as pairs of Fe^{2+} ions coupled antiferromagnetically. In Fig. 4 of Ref. 4 spectra are shown in which additional lines labeled II, III, and IV appear. These originate from transitions between thermally populated excited states of the $^5\Gamma_3$ multiplet and the lowest Γ_5 level of the $^5\Gamma_5$ multiplet. Again, associated with line II there is a line, $X_{\rm II}$, which bears the same relation to II as $X_{\rm I}$ does to I. Thus, we conclude that $X_{\rm I}$ and $X_{\rm II}$ share the same final state.

In this work we attribute the X and Y absorption lines to transitions from states in the $^5\Gamma_3$ multiplet to vibronic states associated with the $^5\Gamma_5$ multiplet. The Fe^{2+} states in the upper multiplet can interact with Γ_5 and Γ_3 phonons while the states in $^5\Gamma_3$ can only couple with Γ_3 phonons. In principle, all phonons of these symmetries should be considered regardless of their origin in the BZ when described as traveling waves. However, according to Ham, Schwarz, and O'Brien,[9] it is often a good approximation to replace the spectrum with a single phonon of each kind whose frequencies are suitable averages over the whole phonon bands.

TABLE I. Phonon modes at high symmetry points in the Brillouin zone, their decomposition according to the point group of the site and their energies for CdTe.

Phonon modes	T_d decomposition	Energy (cm^{-1})	Source
TA(X)	$\Gamma_4\oplus\Gamma_5$	35.0	a
LA(X)	Γ_5	125.0	a
TO(X)	$\Gamma_4\oplus\Gamma_5$	148.7	a
LO(X)	$\Gamma_1\oplus\Gamma_3$	133.3	b
TA(L)	$\Gamma_3\oplus\Gamma_4\oplus\Gamma_5$	29.3	a
LA(L)	$\Gamma_1\oplus\Gamma_5$	108.3	a
TO(L)	$\Gamma_3\oplus\Gamma_4\oplus\Gamma_5$	144.3	a
LO(L)	$\Gamma_1\oplus\Gamma_5$	144.3	a
TA$_1$(K)	$\Gamma_2\oplus\Gamma_3\oplus2\Gamma_4\oplus\Gamma_5$	36.7	a
TA$_2$(K)	$\Gamma_1\oplus\Gamma_3\oplus\Gamma_4\oplus2\Gamma_5$	52.7	a
LA(K)	$\Gamma_1\oplus\Gamma_3\oplus\Gamma_4\oplus2\Gamma_5$	105.4	b

[a]J. M. Rowe, R. M. Nicklow, D. L. Prince, and K. Zanio, Phys. Rev. B 10, 671 (1974).
[b]*Numerical Data and Functional Relationships in Science and Technology,* edited by O. Madelung, M. Schulz, and H. Weiss Landolt-Börnstein, New Series, Group III, Vol. 17, Pt. b (Springer, Berlin, 1982), pp. 227, 319, and 459.

We note that, in the spectrum in Fig. 2 of Ref. 4, the structure to the left of the Y line can be interpreted as electronic transitions of type I accompanied by emission of phonons identified with modes at several high symmetry points in the BZ. However, the transverse acoustic phonons (TA) appear to be absent from these features. The presence of TA phonons at the X, L, and K points of the BZ possessing Γ_5 symmetry in their decompositions suggests the consideration of vibronic states resulting from the interaction of electronic levels of the $^5\Gamma_5$ multiplet with TA (Γ_5) phonons and their overtones.

Ham[10] has shown that a Jahn-Teller coupling stronger than the spin-orbit interaction can lead to a drastic reduction of the separation of the levels deduced from crystal-field theory. In a study of the $^4\Gamma_4$ *orbital* multiplet of Co^{2+} in ZnSe, Uba and Baranowski[11] have worked out the vibronic states formed by the electron levels interacting with a phonon mode of symmetry Γ_3 and its overtones. They considered a TA (Γ_3) phonon of energy $\hbar\omega=72$ cm^{-1} at X in the BZ where the density of phonon states exhibits a peak. Coupling this phonon and its overtones up to order 20 with the $^4\Gamma_4$ Co^{2+} orbital levels, they obtained vibronic states separated by considerable less energy than $\hbar\omega$. In fact, for a sufficiently strong Jahn-Teller energy this difference in energy can even approach zero.

In Sec. III we consider vibronic states resulting from the coupling of the $^5\Gamma_5$ levels with a single-phonon mode of symmetry Γ_5. We use for the Jahn-Teller energy the value $E_{JT}=255\ \mathrm{cm}^{-1}$ deduced for $Cd_{1-x}Fe_xTe$ by Slack, Ham, and Chrenko.[3] However, in our study both E_{JT} and the phonon energy $\hbar\omega$ were adjusted to obtain the best fit to the positions of the X_I and Y lines. This was achieved with the value of E_{JT} just quoted and $\hbar\omega\approx 40\ \mathrm{cm}^{-1}$. The number of phonons in the overtones was varied up to $N=12$, a value for which satisfactory convergence was achieved for the lower eigenvalues in the $^5\Gamma_5$ manifold.

We also investigated the possible formation of vibronic states by Γ_3 phonons interacting with the $^5\Gamma_3$ multiplet of Fe^{2+} in an attempt to account for a feature observed in transmission in line II of $Cd_{1-x}Fe_xTe$ for a thin sample having a Fe^{2+} concentration of $1.0\times 10^{19}\ \mathrm{cm}^{-3}$. This feature appears in Fig. 6(b) of Ref. 4 where line II shows a clear splitting of about two wave numbers. In order to account for this separation in terms of the Jahn-Teller effect it was necessary to take $\hbar\omega=29.3\ \mathrm{cm}^{-1}$, corresponding to a TA($L$) mode and $E_{JT}=26.4\ \mathrm{cm}^{-1}$, a value much larger than that considered by previous authors.[12,13] This hypothesis becomes untenable, particularly in the light of the additional changes in the spectrum that would be required and would alter the agreement between crystal-field theory and the observations of Ref. 4. Furthermore, since such an hypothesis would alter the ordering of the levels in the $^5\Gamma_3$ manifold, the agreement between theory and experiment[14–16] with regard to the anisotropy of the nonlinear magnetization of $Cd_{1-x}Fe_xTe$ in strong magnetic fields would have to be abandoned. Other choices of the phonon energy and of E_{JT} proved equally unsuccessful. Thus, we conclude that the splitting of line II mentioned above cannot be attributed to a Jahn-Teller effect.

II. ELECTRIC-DIPOLE TRANSITIONS BETWEEN STATES IN THE 3D CONFIGURATION OF Fe^{2+}

Electric-dipole transitions between $3d^6$ levels in the free Fe^{2+} ion are forbidden by parity considerations. However, in a zinc-blende crystal the parity nonconserving part of the T_d potential, namely $a_3'\sum_a x_a y_a z_a$, mixes the $3d^6$ states with configurations of odd parity and, thereby, renders $3d^6\to 3d^6$ transitions electric-dipole allowed. In order to estimate the oscillator strengths of the observed absorption lines we consider here mixing of the orbital $^5\Gamma_3$ and $^5\Gamma_5$ states of $3d^6$ with states in the $3d^5 4p$ and $3d^5 4f$ configurations only. We shall disregard the splittings of the terms in the latter two configurations under the influence of the crystal potential because the resulting energy separations are small compared to their energies measured from the ground state. We shall even neglect the energy separations between the different terms in those configurations because terms in the $3d^5 4p$ configuration lie above $3d^6$ by about $1.2\times 10^5\ \mathrm{cm}^{-1}$ and the energy of a typical $3d^5 4f$ term is $\sim 1.9\times 10^5\ \mathrm{cm}^{-1}$ above the ground state of the ion, these energies being large compared with the term splittings.

Denoting by $\mathbf{A}$ the vector potential of the incident radiation, and by $-e$, m, and c the charge and mass of the electron and the speed of light, respectively, the photon-ion interaction is

$$\frac{e}{mc}\mathbf{A}\cdot\sum_a \mathbf{p}_a\ , \tag{4}$$

where $\mathbf{p}_a$ is the momentum operator of the ath electron. The matrix element of $\mathbf{p}=\sum_a \mathbf{p}_a$ between the states $|l^n;LS,M_L M_s\rangle$ and $|l^{n-1}(L_1S_1)l';L'S',M_L'M_S'\rangle$ is given by[17]

$$\left\langle l^{n-1}(L_1S_1)l';L'S',M_L'M_S'\left|\sum_a \mathbf{p}_a\right|l^n;LS,M_LM_S\right\rangle = n^{1/2}\langle l^{n-1}(L_1S_1)l;LS|\}l^n;LS\rangle$$
$$\times\langle l^{n-1}(L_1S_1)l';L'S',M_L'M_S'|\mathbf{p}_1|l^{n-1}(L_1S_1)l;LS,M_LM_S\rangle\ . \tag{5}$$

Here $|l^n;LS,M_LM_S\rangle$ is a state in the LS term of the n-electron l^n configuration (for $3d^6$, $l=2$, $n=6$), M_L and M_S are the eigenvalues of the projections of the operators $\mathbf{L}$ and $\mathbf{S}$ on an arbitrary direction (usually denoted by $\hat{z}$, in this paper we shall take $\hat{z}$ along one of the cubic axes of the crystal) and $|l^{n-1}(L_1S_1)l';L'S',M_L'M_S'\rangle$ is a state in the $L'S'$ term of a configuration obtained adding a l' electron to the L_1S_1 term of the l^{n-1} configuration. The symbol $\langle l^{n-1}(L_1S_1)l;LS|\}l^n;LS\rangle$ stands for a coefficient of fractional parentage (cfp). The cfp's are the prefactors in the expansion of a wave function belonging to the LS term in a l^n configuration as a linear combination of those resulting from the addition of a l electron to the L_1S_1 term of the l^{n-1} configuration. Tabulations of the coefficients of fractional parentage for d^n configurations have been given by Racah[17] and are also quoted by Slater[18] for $n\le 5$. For $n>5$ we use the relation[17]

$$\langle l^{4l+1-n}(L'S')l;LS|\}l^{4l+2-n};LS\rangle = (-1)^{L+L'+S+S'-l-(1/2)}\left[\frac{(n+1)(2L'+1)(2S'+1)}{(4l+2-n)(2L+1)(2S+1)}\right]^{1/2}$$
$$\times\langle l^n(LS)l;L'S'|\}l^{n+1};L'S'\rangle\ . \tag{6}$$

Equation (5) reduces the calculation of the matrix elements of $\sum_a \mathbf{p}_a$ to that of a single-electron operator, in this case, say, $\mathbf{p}_1$. We note that, even though Eq. (5) is written for the total electron momentum, it is valid for any symmetric operator of one-electron observables. This result can now be applied to the crystal potential which may be expanded in terms of irreducible tensor components as

$$V(\mathbf{r})=\sum_{k=0}^{\infty}\sum_{\kappa=-k}^{k} A_{\kappa}^{(k)}V_{\kappa}^{(k)}(\mathbf{r}) \; . \tag{7}$$

Since we are considering mixing of ${}^5D(3d^6)$ with $3d^54p$ and $3d^54f$ we keep only the odd xyz term in $V(\mathbf{r})$. But $xyz=-i(2\pi/105)^{1/2}r^3[Y_3^2(\theta,\phi)-Y_3^{-2}(\theta,\phi)]$ so that we set $A_2^{(3)}=-ia_3'(2\pi/105)^{1/2}=A_{-2}^{(3)*}$ and $V_{\pm 2}^{(3)}(\mathbf{r})=r^3Y_3^{\pm 2}(\theta,\phi)$. We note that $V(\mathbf{r})$ does not depend on spin so that we need only consider terms with $S=2$. Furthermore, as indicated in Eq. (5), the matrix elements of $\sum_a \mathbf{p}_a$ as well as those of $\sum_a V(\mathbf{r}_a)$ are diagonal in the quantum numbers M_S and independent of their values. Since $V_{\pm 2}^{(3)}$ behave as F functions, it appears, at first sight, that we are required to mix the ${}^5D$ states with terms having $L'=1$, 2, 3, 4, and 5. However, since we only require the matrix elements of $\mathbf{p}$ between perturbed states it is enough to restrict L' to 1, 2, and 3.

The matrix elements of $\sum_a V_{\kappa}^{(k)}(\mathbf{r}_a)$ are obtained with the aid of the Racah formalism and the Wigner-Eckart theorem. Omitting M_S and M_S', which, for nonvanishing elements must be equal, we have

$$\left\langle l^n;{}^{2S+1}LM_L \left| \sum_a V_{\kappa}^{(k)}(\mathbf{r}_a) \right| l^{n-1}({}^{2S_1+1}L_1)l';{}^{2S+1}L'M_L' \right\rangle$$
$$=(-1)^{M_L+L_1-l+1}\langle l^n;LS\{|l^{n-1}(L_1S_1)l;LS\rangle[n(2L+1)(2L'+1)]^{1/2}$$
$$\times\langle l\|V^{(k)}\|l'\rangle W(lLl'L';L_1k)\begin{bmatrix} L & L' & k \\ -M_L & M_L' & \kappa \end{bmatrix} . \tag{8}$$

In Eq. (8) the terms are designated by ${}^{2S+1}L$ and the last three factors are, respectively, the reduced matrix element of $V_{\kappa}^{(k)}=r^kY_k^{\kappa}(\theta,\phi)$ which appears in its usual form in the Wigner-Eckart theorem, the Racah coefficient $W(lLl'L';L_1k)$ and a $3j$ symbol. The quantity $\langle l\|V^{(k)}\|l'\rangle$ is equal to the product of $\langle l|r^k|l'\rangle$ and $\langle l|Y^{(k)}|l'\rangle$ where $\langle l|r^k|l'\rangle$ is the matrix element of r^k between radial wave functions[19] corresponding to angular momenta l and l' and $\langle l\|Y^{(k)}\|l'\rangle$ is the reduced matrix element[20] of a spherical harmonic of order k. The pertinent terms in the $3d^54p$ and $3d^54f$ configurations, the appropriate cfp's and the Racah coefficients necessary to calculate the matrix elements of $V_{\pm 2}^{(3)}$ and $\mathbf{p}$ between these terms and the ground term, $3d^6({}^5D)$, are listed in Tables II and III. The orbital ${}^5\Gamma_3$ states of the ${}^5D$ term are $\gamma_1=|0\rangle$ and $\gamma_2=2^{-1/2}(|2\rangle+|-2\rangle)$ which behave as $2z^2-x^2-y^2$ and $\sqrt{3}(x^2-y^2)$, respectively. Similarly, the ${}^5\Gamma_5$ orbitals are $\epsilon_1=-2^{-1/2}(|1\rangle+|-1\rangle)$, $\epsilon_2=i2^{-1/2}(|-1\rangle-|1\rangle)$, and $\epsilon_3=2^{-1/2}(|2\rangle-|-2\rangle)$ which behave as yz, zx, and xy, respectively. Here $|M_L\rangle$ designates the eigenvectors of L_z for $L=2$ ($M_L=2,1,0,-1,-2$). To calculate the oscillator strength for a transition ${}^5\Gamma_3\rightarrow{}^5\Gamma_5$ we consider the z component of $\mathbf{p}$. The cubic symmetry ensures that that is all that is required. Since $p_z|\gamma_1\rangle$ belongs to the third row of Γ_5 it is enough to calculate $\langle\epsilon_3|p_z|\gamma_1\rangle$. However, we need to obtain the mixed states $\tilde{\gamma}_1$ and $\tilde{\epsilon}_3$ from standard perturbation theory.[21] We find

$$\langle\tilde{\epsilon}_3|p_z|\tilde{\gamma}_1\rangle=\sum_i\left[\frac{\langle\epsilon_3|p_z|i\rangle\left\langle i\left|\sum_a V(\mathbf{r}_a)\right|\gamma_1\right\rangle}{E_{\gamma}-E_i}+\frac{\left\langle\epsilon_3\left|\sum_a V(\mathbf{r}_a)\right|i\right\rangle\langle i|p_z|\gamma_1\rangle}{E_{\epsilon}-E_i}\right] . \tag{9}$$

We now use

$$\left[H_0,\sum_a z_a\right]=-(i\hbar/m)p_z \; ,$$

TABLE II. Terms in the $3d^54p$ configuration needed for the analysis of the oscillator strength of ${}^5\Gamma_3\rightarrow{}^5\Gamma_5$ transitions of Fe^{2+} in a tetrahedral field. The appropriate coefficients of fractional parentage (cfp) and Racah coefficients are displayed.

Term ${}^5L'({}^{2S_1+1}L_1)$	cfp $\langle d^6;{}^5D\{|d^5({}^{2S_1+1}L_1)d;{}^5D\rangle$	Racah coefficients $W(221L';L_11)$	$W(221L';L_13)$
${}^5P({}^6S)$	$5^{-1/2}$	$15^{-1/2}$	$15^{-1/2}$
${}^5P({}^4P)$	$-10^{-1/2}$	$-20^{-1/2}$	$45^{-1/2}$
${}^5P({}^4D)$	$6^{-1/2}$	$10^{-1}(\frac{7}{3})^{1/2}$	$5^{-1}(21)^{-1/2}$
${}^5D({}^4P)$	$-10^{-1/2}$	10^{-1}	$5^{-1}(\frac{2}{3})^{1/2}$
${}^5D({}^4D)$	$6^{-1/2}$	$-10^{-1}(\frac{7}{3})^{1/2}$	$5^{-1}(\frac{2}{7})^{1/2}$
${}^5D({}^4F)$	$-(\frac{7}{30})^{1/2}$	$5^{-1}(\frac{2}{3})^{1/2}$	35^{-1}
${}^5F({}^4D)$	$6^{-1/2}$	$5^{-1}(21)^{-1/2}$	$(\frac{2}{35})6^{-1/2}$
${}^5F({}^4F)$	$-(\frac{7}{30})^{1/2}$	$-(105)^{-1/2}$	$7^{-1}(\frac{3}{10})^{1/2}$
${}^5F({}^4G)$	$(\frac{3}{10})^{1/2}$	$(35)^{-1/2}$	$(21)^{-1}(10)^{-1/2}$

TABLE III. Terms in the $3d^54f$ configuration needed for the calculation of the oscillator strength of ${}^5\Gamma_3 \rightarrow {}^5\Gamma_5$ transitions of Fe^{2+} in a tetrahedral field. The appropriate coefficients of fractional parentage (cfp) and Racah coefficients are displayed.

Term ${}^5L'({}^{2S_1+1}L_1)$	cfp $\langle d^6;{}^5D\{\|d^5({}^{2S_1+1}L_1)d;{}^5D\rangle$	Racah coefficients $W(223L';L_11)$	$W(223L';L_13)$
${}^5P({}^4D)$	$6^{-1/2}$	$5^{-1}(21)^{-1/2}$	$(\frac{2}{35})6^{1/2}$
${}^5P({}^4F)$	$-(\frac{7}{30})^{1/2}$	$-(105)^{-1/2}$	$7^{-1}(\frac{3}{10})^{1/2}$
${}^5P({}^4G)$	$(\frac{3}{10})^{1/2}$	$(35)^{-1/2}$	$(21)^{-1}10^{-1/2}$
${}^5D({}^4P)$	$-10^{-1/2}$	-15^{-1}	$-5^{-1}(\frac{3}{7})^{1/2}$
${}^5D({}^4D)$	$6^{-1/2}$	$5^{-1}(\frac{2}{7})^{1/2}$	$(70)^{-1}6^{1/2}$
${}^5D({}^4F)$	$-(\frac{7}{30})^{1/2}$	$-5^{-1}(\frac{3}{7})^{1/2}$	10^{-1}
${}^5D({}^4G)$	$(\frac{3}{10})^{1/2}$	$3^{-1}(7^{-1/2})$	$(14)^{-1}3^{-1/2}$
${}^5F({}^6S)$	$5^{-1/2}$	$(35)^{-1/2}$	$(35)^{-1/2}$
${}^5F({}^4P)$	$-10^{-1/2}$	$-(\frac{2}{3})(\frac{2}{35})^{1/2}$	$-2^{-1}(70)^{-1/2}$
${}^5F({}^4D)$	$6^{-1/2}$	$(\frac{2}{35})6^{1/2}$	$-(\frac{11}{70})6^{-1/2}$
${}^5F({}^4F)$	$-(\frac{7}{30})^{1/2}$	$-(7^{-1})(\frac{3}{5})^{1/2}$	$(\frac{2}{7})15^{-1/2}$
${}^5F({}^4G)$	$(\frac{3}{10})^{1/2}$	$(21)^{-1}(\frac{11}{5})^{1/2}$	$(21)^{-1}(\frac{11}{5})^{1/2}$

where H_0 is the Hamiltonian whose eigenvectors are $|i\rangle$, γ_1 and ϵ_3 (see Ref. 21), and the completeness of the intermediate states $|i\rangle$ to obtain

$$\langle\tilde{\epsilon}_3|p_z|\tilde{\gamma}_1\rangle=\frac{2\pi m\,\Delta a_3'}{3\hbar\sqrt{35}}\left[\sum_i (E_\gamma-E_i)^{-1}\langle 2|Z_0^{(1)}|i\rangle\langle i|U_2^{(3)}|0\rangle+(E_\epsilon-E_i)^{-1}\langle 2|U_2^{(3)}|i\rangle\langle i|Z_0^{(1)}|0\rangle+\text{c.c.}\right]. \quad (10)$$

In Eq. (10)

$$U_2^{(3)}=\sum_a r_a^3 Y_3^2(\theta_a,\phi_a)=\sum_a V_2^{(3)}(\mathbf{r}_a) \quad (11)$$

and

$$Z_0^{(1)}=\sum_a r_a Y_1^0(\theta_a,\phi_a)=(3/4\pi)^{1/2}\sum_a z_a\ . \quad (12)$$

These results are obtained after replacing ϵ_3 by its value in terms of $|M_L\rangle$ and collecting the terms involving $U_2^{(3)}$ and $U_{-2}^{(3)}$ using the properties of the matrix elements.[22] For intermediate levels in the $3d^54p$ and $3d^54f$ configurations, the energy difference between E_i-E_γ and E_i-E_ϵ, namely Δ, is small compared to the quantities themselves and, furthermore, a small error is made if we disregard the energy differences between the terms in each of the above configurations. Thus, in the summation over intermediate states in Eq. (10) we can replace the energy denominators by ΔE_{dp} and ΔE_{df}, the average energies above the ground state of the $3d^54p$ and $3d^54f$ configurations. These quantities are,[23] approximately, $1.2\times10^5\ \text{cm}^{-1}$ and $1.9\times10^5\ \text{cm}^{-1}$, respectively for Fe^{2+}. With these approximations we can write

$$\langle\tilde{\epsilon}_3|p_z|\tilde{\gamma}_1\rangle\approx\frac{2m\,\Delta a_3'}{35\hbar\sqrt{3}}\times\left[-\frac{\langle 3d|r|4p\rangle\langle 4p|r^3|3d\rangle}{\Delta E_{dp}}+\frac{\langle 3d|r|4f\rangle\langle 4f|r^3|3d\rangle}{\Delta E_{df}}\right]. \quad (13)$$

The contributions to the transition matrix elements from virtual excitations of states in higher configurations such as $3d^55p$ and $3d^55f$ can be neglected because their effective radii exceed the anion-cation distance (thereby becoming inappropriate energy levels of the ion in the crystal host) and their energies above the ground state are larger than those considered above. The oscillator strength of the $\gamma_1\rightarrow\epsilon_3$ transition is

$$f_{\gamma\rightarrow\epsilon}=\frac{2m\Delta}{\hbar^2}\left|\left\langle\tilde{\epsilon}_3\left|\sum_a z_a\right|\tilde{\gamma}_1\right\rangle\right|^2 \simeq\frac{8m\,\Delta a_3'^2}{3675\hbar^2}\left[\frac{\langle 3d|r|4p\rangle\langle 4p|r^3|3d\rangle}{\Delta E_{dp}}-\frac{\langle 3d|r|4f\rangle\langle 4f|r^3|3d\rangle}{\Delta E_{df}}\right]^2. \quad (14)$$

An estimate of the matrix elements of r and r^3 between the radial wave functions $|3d\rangle$ and $|4p\rangle$ on the one hand and $|3d\rangle$ and $|4f\rangle$ on the other can be given as follows. Using the experimentally measured ionization energies of Fe^{2+} and equating them to $\text{Ry}(z^*/n)^2$ where Ry is the Rydberg and n the principal quantum number of a particular state we find an effective charge z^* for each level. This charge can be viewed as the combined effect of the nuclear charge and of the screening of the remaining electrons in the ion and equals 4.502, 4.305 and 2.886 for the $3d$, $4p$, and $4f$ electrons, respectively. Using hydrogen-like radial wave functions (modified by the effective charge z^*e) we obtain

$$\langle 3d|r^3|4p\rangle\langle 4p|r|3d\rangle = 2.581$$

and

$$\langle 3d|r^3|4f\rangle\langle 4f|r|3d\rangle = 34.793$$

in atomic units.

In the point ion model $a_3' = (20/\sqrt{3})(ze^2/R^4)$ where, as before, z is the ionic charge and R the anion-cation nearest-neighbor distance. The oscillator strength is

$$(64z^2\Delta/441R^8)[(\Delta E_{dp})^{-1}\langle 3d|r|4p\rangle\langle 4p|r^3|3d\rangle - (\Delta E_{df})^{-1}\langle 3d|r|4f\rangle\langle 4f|r^3|3d\rangle]^2 ,$$

where it is understood that all quantities are expressed in atomic units ($\Delta = 0.011\,25$, $R = 5.2912$, $\Delta E_{dp} = 0.5468$, $\Delta E_{df} = 0.8657$). We obtain $f_{\gamma\rightarrow\epsilon} = 1.3\times 10^{-5}$. If we assume that the charge density, being partly covalent in origin, possesses a center of charge at $R \approx 2$ Å obtained from the ratio of a_4' deduced from experiment instead of from the point ion hypothesis, $f_{\gamma\rightarrow\epsilon}$ becomes of the order of 2×10^{-4}. The experimentally estimated value of the oscillator strength[1] is 2.9×10^{-5}. It must however be borne in mind that our calculated value represents the total oscillator strength of the transitions from $^5\Gamma_3$ to $^5\Gamma_5$ so that the agreement between measured and calculated values of the oscillator strength is rather satisfactory.

III. VIBRONIC STATES

As mentioned in the Introduction, the second objective of this work is to provide a possible mechanism to account for the X and Y lines in the near infrared spectrum[4] of $Cd_{1-x}Fe_xTe$. We investigate the consequences of the assumption that there exists a strong coupling between the $Fe^{2+}\,{}^5\Gamma_5$ manifold and a Γ_5 phonon.

In first order of the atomic displacements, the electron-phonon interaction can be expressed in the general form

$$H_{ep} = \sum_a \sum_{\alpha v\lambda} V_{v\lambda}^{(\alpha)}(\mathbf{r}_a) Q_{v\lambda}^{(\alpha)} . \tag{15}$$

Here, the normal coordinates $Q_{v\lambda}^{(\alpha)}$ of the vibrational modes and the electronic operators are classified according to the irreducible representations of the group of the lattice site occupied by the magnetic ion. In Eq. (15) Γ_v denotes one of the irreducible representations of the group (to fix the ideas, in our case this group is T_d), λ is one of the rows of the representation Γ_v ($\lambda = 1,2,\ldots,l_v$) and α is an index corresponding to the enumeration of the possible modes having symmetry Γ_v. The expectation value of H_{ep} vanishes in a non-degenerate electronic state since the complete Born-Oppenheimer vibrational energy is of second order in the atomic displacements. However, the matrix associated with H_{ep} for a degenerate level possesses, in general, nonvanishing, off-diagonal elements which may lead to a splitting of the energy levels. Consider, e.g., a level belonging to Γ_v with degeneracy $l_v > 1$ and denote the orthonormal electronic states by $\psi_{i\kappa}$ (i labels the irreducible representation Γ_i of the level and $\kappa = 1,2,\ldots,l_i$, the particular row to which $\psi_{i\kappa}$ belongs). The potential energy as a function of $Q_{i\lambda}^{(\alpha)}$ ($\lambda = 1,2,\ldots,l_v$) has a minimum when all Q's vanish. We denote this energy by $U_0(Q)$. The matrix elements of H_{ep} between $\psi_{i\kappa}$ and $\psi_{i\kappa'}$ are

$$\langle\psi_{i\kappa'}|H_{ep}|\psi_{i\kappa}\rangle = \sum_{\alpha v\lambda} V_{iv}^{(\alpha)} Q_{v\lambda}^{(\alpha)} \langle\Gamma_i\kappa'|\Gamma_v\Gamma_i;\lambda\kappa\rangle . \tag{16}$$

Here $V_{iv}^{(\alpha)}$ is a reduced matrix element depending on Γ_i and Γ_v only and not on the row indices λ, κ, and κ'. All dependences on these indices is contained in the Clebsch-Gordan coefficients (called coupling coefficients by Koster *et al.*[5]) of the group written here in the form $\langle\Gamma_i\kappa'|\Gamma_v\Gamma_i;\lambda\kappa\rangle$. These are determined unambiguously if the group is simply reducible which is, in fact, the case for the single-valued representations of T_d. The matrix Hamiltonian for the whole system is

$$\langle\psi_{i\kappa'}|H|\psi_{i\kappa}\rangle = U_0(Q)\delta_{\kappa'\kappa} + \sum_{\alpha v\lambda} V_{iv}^{(\alpha)} Q_{v\lambda}^{(\alpha)} \langle\Gamma_i\kappa'|\Gamma_v\Gamma_i;\lambda\kappa\rangle . \tag{17}$$

The new eigenstates are obtained diagonalizing the matrix (17). To each eigenstate there is associated a potential energy surface in Q space which, because H_{ep} is linear in the coordinates $\mathbf{Q}$, possesses, in general, several minima at positions other than $\mathbf{Q}=\mathbf{0}$. The arrangement of atoms is then distorted with respect to that in the high symmetry configuration giving rise to the Jahn-Teller distortion.

For example, consider a single (degenerate) phonon level of symmetry Γ_v. The matrix (17) takes the form

$$H^{(i)} = \sum_\lambda \left[\frac{P_\lambda^2}{2\mu} + \frac{1}{2}\mu\omega^2 Q_\lambda^2\right] + V\sum_\lambda Q_\lambda M_\lambda = \sum_\lambda \hbar\omega(a_\lambda^\dagger a_\lambda + \tfrac{1}{2}) + K\sum_\lambda (a_\lambda^\dagger + a_\lambda) M_\lambda . \tag{18}$$

Here P_λ is the momentum variable canonically conjugated with Q_λ, μ an appropriate reduced mass and $a_\lambda (a_\lambda^\dagger)$, a destruction (creation) operator of a phonon belonging to the λ row of Γ_v. V is the coupling constant which, by convention, is selected positive, M_λ is the matrix formed by the Clebsch-Gordan coefficients $\langle\Gamma_i\kappa'|\Gamma_v\Gamma_i;\lambda\kappa\rangle$ for each λ. The parameter K equals $V(\hbar/2\mu\omega)^{1/2}$.

For an electronic level belonging to the Γ_5 irreducible representation of T_d interacting with a Γ_5 phonon,

$$M_1 = 2^{-1/2}\begin{bmatrix} 0 & 0 & 0 \\ 0 & 0 & 1 \\ 0 & 1 & 0 \end{bmatrix} , \quad M_1 = 2^{-1/2}\begin{bmatrix} 0 & 0 & 1 \\ 0 & 0 & 0 \\ 1 & 0 & 0 \end{bmatrix} , \quad M_3 = 2^{-1/2}\begin{bmatrix} 0 & 1 & 0 \\ 1 & 0 & 0 \\ 0 & 0 & 0 \end{bmatrix} . \tag{19}$$

Here the M_λ ($\lambda = 1,2,3$) are referred to a basis transforming as x,y,z where these are the coordinates of a vector

TABLE IV. Reduction of the completely symmetric representations $[\Gamma_5^N]$ for a $\Gamma_5(T_d)$ phonon $N \le 12$. The coefficients in the reduction $[\Gamma_5^N]=\sum_{i=1}^{5} a_i^{(N)}\Gamma_i$ are listed.

N	$a_1^{(N)}$	$a_2^{(N)}$	$a_3^{(N)}$	$a_4^{(N)}$	$a_5^{(N)}$
1	0	0	0	0	1
2	1	0	1	0	1
3	1	0	0	1	2
4	2	0	2	1	2
5	1	0	1	2	4
6	3	1	3	2	4
7	2	0	2	4	6
8	4	1	5	4	6
9	3	1	3	6	9
10	5	2	7	6	9
11	4	1	5	9	12
12	7	3	9	9	12

referred to the cubic axis. The minima of the potential-energy surfaces equal $-V^2/3\mu\omega$ and occur at $(V\sqrt{2}/3\mu\omega^2)$ along $[\bar{1}11]$, $[1\bar{1}1]$, $[11\bar{1}]$, and $[\bar{1}\bar{1}\bar{1}]$ in **Q** space. The quantity $(V^2/3\mu\omega^2)=(2K^2/3\hbar\omega)=E_{\rm JT}$ is called the Jahn-Teller energy.

The coupling between the electronic and phonon states is carried out as follows. We consider a phonon mode of symmetry Γ_v and degeneracy l_v. The overtones are characterized by the non-negative integers $\{n_\lambda\}$ $(\lambda=1,2,\ldots,l_v)$ and expressed in the form

$$|n_1,n_2,\ldots,n_{l_v}\rangle=\left[\prod_{\lambda=1}^{l_v} n_\lambda!\right]^{-1/2}\prod_{\lambda=1}^{l_v}(a_\lambda^\dagger)^{n_\lambda}|0\rangle \tag{20}$$

where $|0\rangle$ is the zero-phonon state. For an overtone of order $N=\sum_\lambda n_\lambda$, these states generate a representation of the point group obtained by forming the completely symmetric direct product of Γ_v taken N times. For $l_v=3$ this representation is of dimension $(N+1)(N+2)/2$, and is, in general, reducible. Table IV shows the reduction of $[\Gamma_5^N]$ (of T_d) for $N=1,2,\ldots,12$. Using the method of projection operators we also find the symmetrized overtones. The first few are displayed in Table V.

The vibronic states are constructed forming the direct product of the electronic states in the $^5\Gamma_5$ multiplet and symmetrized overtones of the Γ_5 phonon for $N\le 12$. This results in a classification of the vibronic states according to T_d. There are 295, 271, 566, 840, and 864 vibronic states of symmetries Γ_1, Γ_2, Γ_3, Γ_4, and Γ_5, respectively. To study transitions originating from the Γ_1 ground state it is enough to consider $(N\le 12)$ the 864 vibronic states of symmetry Γ_5 and the two zero-phonon states of the same symmetry in the $^5\Gamma_5$ electronic manifold. The classification and the wave functions of the 866 Γ_5 states was obtained by symbolic calculation on a computer using the Clebsch-Gordan coefficients[5] for the point group T_d. The energy eigenvalues and eigenvectors of all the Γ_5 levels were obtained by numerically diagonalizing the 866×866 matrix associated with these states. For the numerical calculation the crystal-field parameters given by Udo *et al.*[4,24] were used and E_{JT} and $\hbar\omega$ were varied in such a manner as to attain agreement with the spacings of the I, X_I, and Y lines in Ref. 4. The value of $E_{\rm JT}=255$ cm^{-1}, deduced by Slack, Ham, and Chrenko,[3] turned out to provide the best fit, was fixed, and $\hbar\omega$ was varied. The best agreement with the spacing of the I, X_I, and Y lines was obtained with $\hbar\omega\approx 40$ cm^{-1} which may be regarded as an average TA phonon energy at high symmetry points in the BZ. Table VI shows the values of the energies obtained and their comparison with the experimental data of Udo *et al.*[4] We note that the diagonalization yields an additional line close to the position of the third transition observed. In analyzing the relative oscillator strengths we shall see that this line reproduces a further feature of the absorption spectrum. In Fig. 1 we show how the first few energy levels obtained depend on the choice of $N_{\rm max}$. The figure shows that for $N_{\rm max}=12$ the energies approach well defined values thereby justifying this selection.

Figure 2 shows the behavior of the first few levels as functions of $E_{\rm JT}$ for $\hbar\omega=39.7$ cm^{-1}. E_1 is the energy of the zero-phonon line corresponding to the lowest Γ_5 level in the $^5\Gamma_5$ manifold and E_i represents the energy of the vibronic states associated with that level. As can be observed in this diagram the energy levels exhibit a linear behavior as a function of $E_{\rm JT}$ for small values of this energy but become strongly nonlinear for values of $E_{\rm JT}>200$ cm^{-1}. This means that for $E_{\rm JT}\approx 255$ cm^{-1} a

TABLE V. Symmetrized overtones of a $\Gamma_5(T_d)$ phonon of order N $(0\le N\le 3)$.

N	Irreducible representation	State
0	Γ_1	$\|0,0,0\rangle$
1	Γ_5	$\|1,0,0\rangle,\|0,1,0\rangle,\|0,0,1\rangle$
2	Γ_1	$(1/\sqrt{3})(\|2,0,0\rangle+\|0,2,0\rangle+\|0,0,2\rangle)$
2	Γ_3	$(1/\sqrt{6})(\|2,0,0\rangle+\|0,2,0\rangle-2\|0,0,2\rangle)$, $(1/\sqrt{2})(\|0,2,0\rangle-\|2,0,0\rangle)$
2	Γ_5	$\|0,1,1\rangle,\|1,0,1\rangle,\|1,1,0\rangle$
3	Γ_1	$\|1,1,1\rangle$
3	Γ_4	$(1/\sqrt{2})(\|1,2,0\rangle-\|1,0,2\rangle),(1/\sqrt{2})(\|0,1,2\rangle-\|2,1,0\rangle)$, $(1/\sqrt{2})(\|2,0,1\rangle-\|0,2,1\rangle)$
3	Γ_5	$(1/\sqrt{2})(\|1,2,0\rangle+\|1,0,2\rangle),(1/\sqrt{2})(\|2,1,0\rangle+\|0,1,2\rangle)$, $(1/\sqrt{2})(\|0,2,1\rangle+\|2,0,1\rangle)$
3	Γ_5	$\|3,0,0\rangle,\|0,3,0\rangle,\|0,0,3\rangle$

TABLE VI. Experimental positions of line I and three additional lines (X_I, Y, unlabeled) in the absorption spectrum of $Cd_{1-x}Fe_xTe$ compared with the result obtained for transitions from the ground state to the lowest zero-phonon Γ_5 line in the $^5\Gamma_5$ manifold (line I) and the vibronic levels resulting from strong coupling with a $\Gamma_5(T_d)$ phonon. The phonon energy is $\hbar\omega = 40$ cm^{-1} and the Jahn-Teller energy, $E_{JT} = 255$ cm^{-1}.

Observed transitions[a] (cm^{-1})	Calculated transitions (cm^{-1})
2282.8	2282.8
2293.8	2295.3
2309.0	2308.2
	2311.9
2317.8	2321.4

[a]See Ref. 4.

perturbative approach to obtain the energy levels is not appropriate and one must turn to a diagonalization over a relative large number of vibronic states to obtain significant results. Figure 3 shows a detail of Fig. 2 showing the lowest-energy vibronic states and their symmetry classifications.

The relative oscillator strengths for transitions from the Γ_1 ground state in the lower $^5\Gamma_3$ multiplet to the calculated vibronic states were obtained next. Since we do not consider vibronic coupling for the lower manifold, the ground state has complete zero-phonon character and, thus, it has nonzero electric-dipole matrix elements with only the zero-phonon part of each of the Γ_5 vibronic states obtained above. It is then a straightforward matter to obtain the relative oscillator strengths by applying the Wigner-Eckart theorem and factoring out the reduced matrix element. Figure 4 shows an histogram of the relative oscillator strength for the whole spectral region considered in this work. In order to relate these values to the observed spectrum we consider only the first few lines and assign to them a Lorentzian line shape with widths estimated from the experimental results. The intensities are those obtained in the calculations presented in this work. The transmission spectrum obtained, adjusted at the single point for energy 2250 cm^{-1}, is shown in Fig. 5 where it is compared to the experimental result of Udo *et al.*[4] As can be seen the agreement is rather satisfactory, particularly since the shoulder on the third line observed, which was not taken into account in the fitting, is also reproduced in the calculated spectrum.

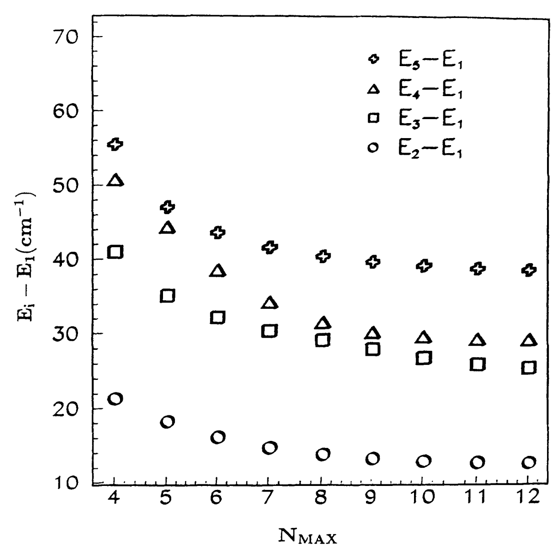

FIG. 1. Energy of the first few vibronic levels as functions of N_{max}, the largest order of the phonon overtones. The phonon energy and E_{JT} were selected equal to 40 and 255 cm^{-1}, respectively. Parameters appropriate for Fe^{2+} in CdTe as given in Ref. 4.

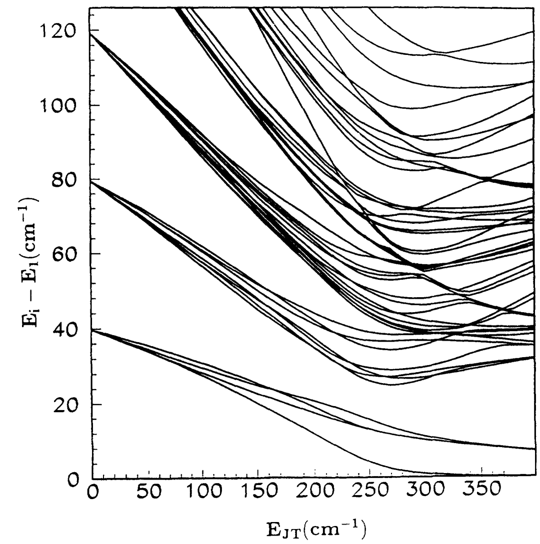

FIG. 2. Variation of the energy difference of the first few vibronic levels belonging to any irreducible representation of T_d of Fe^{2+} in $Cd_{1-x}Fe_xTe$ as functions of the Jahn-Teller stabilization energy E_{JT}. Interaction with a single Γ_5 phonon of energy $\hbar\omega = 40$ cm^{-1} is assumed.

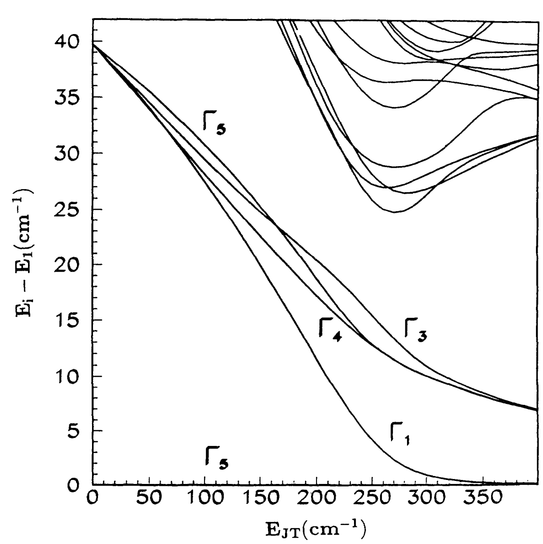

FIG. 3. Detail of the lowest-energy vibronic modes of Fig. 2 including their symmetry classification.

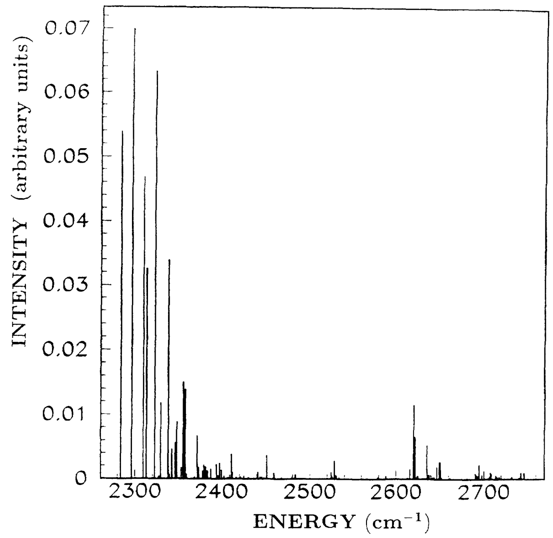

FIG. 4. Histogram of the relative intensities of transitions from the zero-phonon ground state of Fe^{2+} in CdTe to vibronic states associated with the $^5\Gamma_5$ electronic manifold. $N_{max}=12$.

IV. CONCLUDING REMARKS

This paper shows that the experimental estimates of the oscillator strengths of Fe^{2+} in CdTe can be explained by taking into account the mixing by the T_d crystal field of states in the $3d^6$ ^5D term of Fe^{2+} with odd parity states in configurations such as $3d^54p$ and $3d^54f$. Furthermore, we have shown that it is possible to interpret the lines labeled X and Y in the work of Udo *et al.*[4] as resulting from a strong coupling of states in the $^5\Gamma_5$ states with TA phonons of Γ_5 symmetry. The vibronic states of total symmetry Γ_5 yield energy levels lying closer to the lowest electronic, zero-phonon Γ_5 state than would be expected in a simple perturbative approach. This effect can be expected when there is a strong Jahn-Teller stabilization energy.

In Ref. 4 lines X_I and Y were attributed to transitions between states of pairs of Fe^{2+} ions coupled antiferromagnetically on the basis of the dependence of the intensity of the observed lines on Fe^{2+} concentration. The quantum states of pairs of Fe^{2+} are expected to occur in manifolds centered at the approximate energies 0, Δ, and 2Δ where the lowest levels are, arbitrarily, set at zero energy. This result is consistent with a preliminary calculation of the energy levels of Fe^{2+} levels in CdTe assuming an exchange coupling of 30 cm^{-1}. The determination of the transition probabilities is in progress and will allow a quantitative comparison of the two proposed mechanisms for these transitions.

Ham and Slack[25] considered the coupling of the $^5\Gamma_5$ electronic levels of Fe^{2+} in cubic ZnS with Γ_3 phonons. A study by Martinelli, Passaro, and Pastori-Parravicini[26] also makes use of coupling with phonons of Γ_3 symmetry. In the present work we focused on the coupling of the $^5\Gamma_5$ levels of Fe^{2+} with phonons of Γ_5 partly basing our hypothesis on the fact that the coupling of Γ_3 phonons with the $^5\Gamma_3$ states of Fe^{2+} appears to be weak.[27]

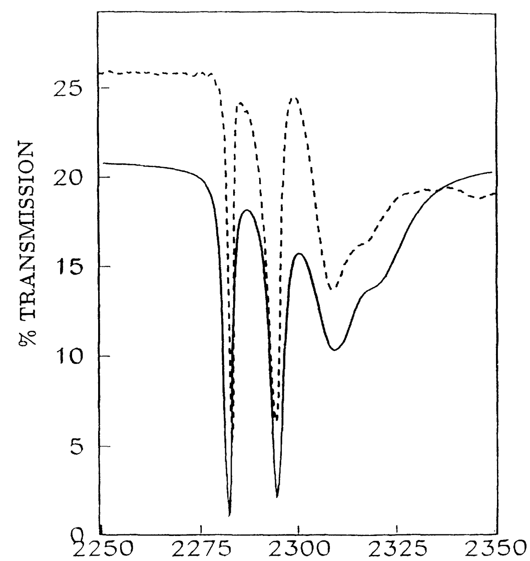

FIG. 5. Comparison of the experimental percent transmission for a sample of $Cd_{1-x}Fe_xTe$ at $T=2$ K (Ref. 4) with the result of the calculations described in the present work. We consider vibronic states originating from the $^5\Gamma_5$ electronic manifold of Fe^{2+} in $Cd_{1-x}Fe_xTe$ and $\Gamma_5(T_d)$ phonons of energy $\hbar\omega=40$ cm^{-1}. $E_{JT}=255$ cm^{-1}. The theoretical result is given by the solid curve. The experimental curve, taken from Ref. 4, is dashed and has been displaced upwards for clarity. The theoretical curve was obtained using the calculated relative absorption coefficient and assuming Lorentzian shapes whose widths equal those of the experimentally observed lines. The relation between the absorption coefficient and the transmission coefficient is $I=I_0(1-R)^2[\exp(\alpha t)-R^2\exp(-\alpha t)]^{-1}$ where R is the reflectivity, and t the thickness of the sample. The experimental curve displayed here and the parameters involved are those in Fig. 3(a) of Ref. 4.

ACKNOWLEDGMENTS

The authors with to thank A. K. Ramdas, G. C. La Rocca, A. J. Mayur, and M. D. Sciacca for many useful discussions on the subject of this paper. We also acknowledge a valuable discussion and correspondence from F. S. Ham. This work was supported by the U.S. National Science Foundation (Grant No. DMR 93-03186) and by Consiglio Nazionale delle Ricerche (Italy) within the framework of its International Cooperation Program. One of the authors (S.R.) wishes to acknowledge the hospitality of the Scuola Normale Superiore (Pisa, Italy) while this work was completed.

[1]See, for example, G. A. Slack, S. Roberts, and J. T. Vallin, Phys. Rev. **187**, 511 (1959).

[2]A review of the field can be found in *Semiconductors and Semimetals,* edited by J. K. Furdyna and J. Kossut (Academic, New York, 1988), Vol. 25.

[3]G. A. Slack, F. S. Ham, and R. M. Chrenko, Phys. Rev. **152**, 376 (1966).

[4]M. K. Udo, M. Villeret, I. Miotkowski, A. J. Mayur, A. K. Ramdas, and S. Rodriguez, Phys. Rev. B **46**, 7459 (1992).

[5]Throughout this paper we use the group-theoretical notation in G. F. Koster, J. O. Dimmock, R. G. Wheeler, and H. Statz, *Properties of the Thirty-Two Point Groups* (MIT, Cambridge, MA, 1966).

[6]See Table I of Ref. 4 for the calculated values of the energy levels of a ^5D term in a tetrahedral field. The values $\Delta=2470$ cm^{-1} and $\lambda=-91$ cm^{-1} for Fe^{2+} in CdTe give a satisfactory account of the observed energy spectrum (see, however, the discussion of the X and Y lines in Sec. III of the present work).

[7]G. Burns, Phys. Rev. **128**, 2121 (1962).

[8]A. Abragam and B. Bleaney, *Electron Paramagnetic Resonance of Transition Ions* (Oxford University Press, London 1970), p. 399.

[9]F. S. Ham, W. M. Schwarz, and M. C. M. O'Brien, Phys. Rev. **185**, 548 (1969).

[10]F. S. Ham, Phys. Rev. **138**, A1727 (1965).

[11]S. M. Uba and J. M. Baranowski, Phys. Rev. B **17**, 69 (1978).

[12]J. T. Vallin, Phys. Rev. B **2**, 2390 (1970).

[13]E. E. Vogel and J. Rivera-Iratchet, Phys. Rev. B **22**, 4511 (1980).

[14]C. Testelin, A. Mauger, C. Rigaux, M. Guillot, and A. Mycielski, Solid State Commun. **71**, 923 (1989).

[15]M. Villeret, S. Rodriguez, and E. Kartheuser, Solid State Commum. **75**, 21 (1990).

[16]M. Villeret, S. Rodriguez, and E. Kartheuser, Phys. Rev. B **43**, 3443 (1991).

[17]G. Racah, Phys. Rev. **63**, 367 (1943).

[18]J. C. Slater, *Quantum Theory of Atomic Structure,* Vol. 2 (McGraw-Hill, New York, 1960).

[19]We remark here that the final result of this analysis is, of course, independent of the choice of phases of the radial wave functions. For convenience we take them to be real. Needless to say $\langle l|r^k|l'\rangle$ depends on the principal quantum numbers as well as on l and l'.

[20]M. Rotenberg, R. Bivins, N. Metropolis, and J. K. Wooten, Jr., *The 3-j and 6-j Symbols* (The Technology Press, Cambridge, MA 1959), p. 5, Eq. (1.22) and pp. 41–53. In this work we need $\langle d\|Y^{(1)}\|p\rangle=(3/2\pi)^{1/2}$, $\langle d\|Y^{(3)}\|p\rangle=-(3/2\sqrt{\pi})$, $\langle d\|Y^{(1)}\|f\rangle=-(3/2\sqrt{\pi})$, $\langle d\|Y^{(3)}\|f\rangle=(7/3\pi)^{1/2}$.

[21]To be precise, the wave functions without the tilde are assumed to be the eigenvectors of the Hamiltonian for the Fe^{2+} ion in the presence of the even part of the crystal field but omitting the spin-orbit interaction. The states $\tilde{\gamma}_1$ and $\tilde{\epsilon}_1$ are the (approximate) eigenvectors of the previous Hamiltonian to which the odd part of the crystal potential has been added.

[22]We note that $\langle i|U_2^{(3)}|0\rangle=\langle 0|U_{-2}^{(3)}|i\rangle^*$ with a similar (and simpler) result for $Z_0^{(1)}$. It turns out that with our choice of wave functions these matrix elements are real. Recall also that $\Delta=E_\epsilon-E_\gamma$.

[23]C. E. Moore, *Atomic Energy Levels,* Natl. Bur. Stand. (U.S.) Circ. No. 467 (U.S. GPO, Washington, D.C., 1952), Vol. 2, p, 60.

[24]It is found that the energy differences do not significantly depend on the precise choice of Δ. The value $\Delta=2536$ cm^{-1} yielded the best fit to the data after the electron-phonon interaction is included.

[25]F. S. Ham and G. A. Slack, Phys. Rev. B **4**, 777 (1971).

[26]L. Martinelli, M. Passaro, and G. Pastori-Parravicini, Phys. Rev. B **39**, 13 343 (1989).

[27]C. Testelin, C. Rigaux, A. Mauger, A. Mycielski, and C. Julien, Phys. Rev. B **46**, 2183 (1992).